Published in final edited form as:
Mol Pharm. 2010 August 2; 7(4): 1223–1234. doi:10.1021/mp100050d.

Enabling the Intestinal Absorption of Highly Polar Anti-Viral Agents: Ion-Pair Facilitated Membrane Permeation of Zanamivir Heptyl Ester and Guanidino Oseltamivir

Jonathan M. Miller[1], **Arik Dahan**[2], **Deepak Gupta**[1], **Sheeba Varghese**[1], and **Gordon L. Amidon**[1,*]

[1]Center for Molecular Drug Targeting, Department of Pharmaceutical Sciences, College of Pharmacy, University of Michigan, Ann Arbor, MI 48109, USA

[2]Department of Clinical Pharmacology, School of Pharmacy, Faculty of Health Sciences, Ben-Gurion University of the Negev, Beer-Sheva 84105, Israel

Abstract

Anti-viral drugs often suffer from poor intestinal permeability, preventing their delivery via the oral route. The goal of this work was to enhance the intestinal absorption of the low-permeability anti-viral agents zanamivr heptyl ester (ZHE) and guanidino oseltamivir (GO) utilizing an ion-pairing approach, as a critical step toward making them oral drugs. The counterion 1-hydroxy-2-napthoic acid (HNAP) was utilized to enhance the lipophilicity and permeability of the highly polar drugs. HNAP substantially increased the log P of the drugs by up to 3.7 log units. Binding constants (K_{11aq}) of 388 M^{-1} for ZHE-HNAP and 2.91 M^{-1} for GO.-HNAP were obtained by applying a quasi-equilibrium transport model to double-reciprocal plots of apparent octanol-buffer distribution coefficients versus HNAP concentration. HNAP enhanced the apparent permeability (P_{app}) of both compounds across Caco-2 cell monolayers in a concentration-dependent manner, as substantial P_{app} ($0.8 – 3.0 \times 10^{-6}$ cm/s) was observed in the presence of 6–24 mM HNAP, whereas no detectable transport was observed without counterion. Consistent with a quasi-equilibrium transport model, a linear relationship with slope near 1 was obtained from a log-log plot of Caco-2 P_{app} versus HNAP concentration, supporting the ion-pair mechanism behind the permeability enhancement. In the rat jejunal perfusion assay, the addition of HNAP failed to increase the effective permeability (P_{eff}) of GO. However, the rat jejunal permeability of ZHE was significantly enhanced by the addition of HNAP in a concentration-dependent manner, from essentially zero without HNAP to 4.0×10^{-5} cm/s with 10 mM HNAP, matching the P_{eff} of the high-permeability standard metoprolol. The success of ZHE-HNAP was explained by its >100-fold stronger K_{11aq} versus GO-HNAP, making ZHE-HNAP less prone to dissociation and ion-exchange with competing endogenous anions and able to remain intact during membrane permeation. Overall, this work presents a novel approach to enable the oral delivery of highly polar anti-viral drugs, and provides new insights into the underlying mechanisms governing the success or failure of the ion-pairing strategy to increase oral absorption.

Keywords

ion-pair; membrane transport; anti-viral; membrane permeability; oral absorption

[*]To whom correspondence should be addressed: College of Pharmacy, University of Michigan, 428 Church St., Ann Arbor, MI 48109-1065, Telephone: (734) 764-2440, Fax: (734) 763-6423, gla.cmdt@umich.edu.

Introduction

Many highly effective drugs suffer from poor intestinal permeability, which limits their oral bioavailability when delivered via the oral route.[1–3] Most orally administered drugs are able to permeate intestinal membranes via the process of passive diffusion, which includes both paracellular and transcellular routes. However, the tremendous selectivity of biological membranes limits the pool of drugs that can be passively transported to those with a relatively narrow range of molecular weight, lipophilicity, and charge state.[4–5] Active uptake via molecular transporters enables some molecules to circumvent cell membranes.[6–9] However, many potential drug candidates are not substrates for these active transport processes. Due to these limitations in cell membrane transport, many promising drug candidates that are highly potent *in-vitro* do not possess adequate cell membrane permeability to be orally active *in-vivo*.

Certain classes of anti-viral agents tend to be polar and highly charged, and as a result, may exhibit poor intestinal membrane permeability and inadequate oral absorption. For example, Zanamivir (ZNV) is an influenza virus neuraminidase inhibitor currently on the market for the treatment of influenza virus types A and B.[10] In addition to being a primary treatment for the common seasonal flu, ZNV has been shown to have therapeutic utility against avian influenza and has emerged as a front-line therapy for the recent Hemagglutinin 1 Neuraminidase 1 (H1N1) global pandemic.[10–11] ZNV is a carboxylic acid that is highly polar and extraordinarily hydrophilic (clogP = −3.63), and therefore lacks sufficient intestinal permeability (percent of oral dose absorbed (%F) = 4%) to allow delivery via the oral route.[10, 12] As a result, ZNV is currently delivered by inhalation, which creates complications and increased risk of bronchospasms in asthma and chronic obstructive pulmonary disease (COPD) patients. Therefore, increasing the intestinal membrane permeability and enabling the oral delivery of ZNV would be a very significant advance.

Guanidino oseltamivir (GO) is another potent anti-viral agent that suffers from poor intestinal membrane permeability and oral absorption[12] The active carboxylate of GO is a very potent influenza virus neuraminidase inhibitor with IC_{50} of 0.9 nM, however, GO is very poorly absorbed (%F = 2%) via the oral route.[12]. GO is the guanidino analog of oseltamivir (OSV), another influenza virus neuraminidase inhibitor that is currently employed as a primary therapy for the common seasonal flu and also the recent H1N1 global pandemic.[10–11] OSV exhibits high oral absorption of 60–80% in humans and is therefore amenable to delivery via the oral route.[12] However, H1N1 influenza has developed increased resistance to OSV, which could limit its effectiveness in the case of a global pandemic.[11] Therefore, alternative OSV analogs such as GO with increased potency and decreased resistance to H1N1 are of interest.

The goal of this work was to enhance the intestinal absorption of the low-permeability anti-viral agents ZNV and GO utilizing an ion-pairing approach, as a critical step toward making them oral drugs. Given the extreme hydrophilicity of ZNV and GO carboxylate, formation of lipophilic esters (e.g ethyl, heptyl esters) do not provide enough increase in lipophilicity to improve intestinal membrane permeation. However, the formation of ester pro-drugs of ZNV and GO carboxylate imparts high positive charge to the molecules by eliminating the negatively charged carboxylate, thus making the ester pro-drugs amenable to ion-pairing with lipophilic counter acids. Therefore, applying the ion-pair approach with a highly lipophilic anion could enable increased intestinal membrane permeation for ester pro-drugs of ZNV and GO carboxylate. In this work, zanamivir heptyl ester (ZHE) was employed as the ester pro-drug of ZNV and GO as the ethyl ester pro-drug of GO carboxylate. The counterion 1-hydroxy-2-napthoic acid (HNAP) was utilized to enhance the lipophilicity and permeability of the highly polar drugs. HNAP makes for an ideal ion-pairing agent as it

possesses high lipophilicity, relatively strong acidity, and it has precedent for use in humans as it is contained in the anti-asthma medication salmeterol xinafoate.[13–14]

Theory

Ion-pair Mediated Octanol-Buffer (pH 6.5) Partitioning

Consider the ion-pair formation between a basic drug and an organic acid in a mixture of octanol and water. Assuming quasi-equilibrium conditions, that is, formation and destruction of ion-pairs as well as octanol-water partitioning processes are near thermodynamic equilibrium, the association constant for ion-pair formation in the aqueous phase, K_{11aq}, is given by:[13–16]

$$K_{11aq}=\frac{[AB]_{aq}}{[A]_{aq}[B]_{aq}} \quad \text{(Equation 1)}$$

Where $[A]_{aq}$, $[B]_{aq}$, and $[AB]_{aq}$, are the aqueous phase concentrations of the organic acid, basic drug, and ion-pair, respectively.

Assuming the total amount of basic drug in the octanol phase, $[B_t]_{oct}$ exists only as ion-pair (i.e $[B_t]_{oct} \approx [AB]_{oct}$), the apparent octanol/aqueous distribution coefficient $D_B = [B_t]_{oct} / [B_t]_{aq}$, of the basic drug can be expressed as:

$$D_B=\frac{[AB]_{oct}}{[B]_{aq}+[AB]_{aq}} \quad \text{(Equation 2)}$$

Where the total amount of basic drug in the aqueous phase $[B_t]_{aq} = [B]_{aq} + [AB]_{aq}$ and $[B]_{aq}$ represents the concentration of free drug in the aqueous phase.

The intrinsic octanol/water partition coefficients for the ion-pair, P_{AB}, can be defined as:

$$P_{AB}=\frac{[AB]_{oct}}{[AB]_{aq}} \quad \text{(Equation 3)}$$

Combining Equations 1, 2, and 3 gives the following relationship:

$$\frac{1}{D_B}=\frac{1}{K_{11_{aq}}P_{AB}[A]_{aq}}+\frac{1}{P_{AB}} \quad \text{(Equation 4)}$$

Where $[A]_{aq} \approx \frac{[A_i]_{aq}}{1+D_A}$ and $[A_i]$ is the initial concentration of organic acid in the aqueous phase before equilibration with octanol, and D_A is the apparent octanol/aqueous distribution coefficient of the organic acid.

Thus, a plot of $\frac{1}{D_B}$ versus $\frac{1}{[A]_{aq}}$ will yield a straight line with $\text{y-intercept}=\frac{1}{P_{AB}}$ and $\text{slope}=\frac{1}{K_{11aq}P_{AB}}$ from which K_{11aq} and P_{AB}, may be ascertained.

The association constant for ion-pair formation in the octanol phase, K_{11oct}, can be expressed as:

$$K_{11_{oct}} = \frac{[AB]_{oct}}{[A]_{oct}[B]_{oct}} \quad \text{(Equation 5)}$$

Where $[A]_{oct}$, $[B]_{oct}$, and $[AB]_{oct}$, are the octanol phase concentration of the organic acid, organic base, and ion-pair, respectively.

Equations 1 and 5 can be combined to give:

$$K_{11oct} = \frac{P_{AB} K_{11_{aq}}}{D_A D_{Bo}} \quad \text{(Equation 6)}$$

Where D_{Bo} is the apparent octanol/aqueous distribution coefficient of the basic drug at pH 6.5, in the absence of ion-pairing agent. Thus, K_{11oct} can be estimated from the experimentally determined values of P_{AB}, K_{11aq}, D_A, and D_{Bo}.

Ion-pair Mediated Membrane Permeation

Consider the rate of permeation, J_{AB}, of an ion-pair through a membrane separating an aqueous donor solution containing the ion-pair and an aqueous receiver solution containing neat solvent. Assuming quasi-equilibrium conditions, J_{AB} can be described by the following equation[13–14, 17–19]

$$J_{AB} = \frac{P_{AB}[AB]_{aq}\mathscr{D}_{AB}A}{L} \quad \text{(Equation 7)}$$

Where $[AB]_{aq}$ represents the concentration of the ion-pair in the aqueous donor phase, $\mathscr{D}_{AB}$ is the diffusivity of the ion-pair in the membrane, A is the cross sectional area of the membrane, and L is the thickness of the membrane.

The intrinsic membrane/aqueous partition coefficient of the ion pair, P_{AB}, can be described by the following equation:

$$P_{AB} = \frac{[AB]_{mem}}{[AB]_{aq}} \quad \text{(Equation 8)}$$

Where $[AB]_{mem}$, represents the concentration of the ion-pair in the membrane.

Likewise, the apparent membrane/aqueous distribution coefficient of the organic acid, D_A and base, D_B can be described by the following equations:

$$D_A = \frac{[A]_{mem}}{[A]_{aq}} \quad \text{(Equation 9)}$$

$$D_B = \frac{[B]_{mem}}{[B]_{aq}} \quad \text{(Equation 10)}$$

Where $[A]_{mem}$ is the concentration of organic acid in the membrane, $[A]_{aq}$ is the concentration of organic acid in the aqueous donor phase, $[B]_{mem}$ is the concentration of organic base in the membrane, and $[B]_{aq}$ is the concentration of organic base in the aqueous donor phase.

The association constant for ion-pair formation in the membrane, K_{11mem}, can be expressed as:

$$K_{11_{mem}} = \frac{[AB]_{mem}}{[A]_{mem}\,[B]_{mem}} \quad \text{(Equation 11)}$$

Equations (7–11) can be combined to express the J_{AB} dependence on $[A]_{aq}$ and $[B]_{aq}$:

$$\log J_{AB} = \log[A]_{aq} + \log[B]_{aq} + \log\left(\frac{K_{11mem} D_A D_B \mathscr{D}_{AB} A}{L}\right) \quad \text{(Equation 12)}$$

When $[A]_{aq} = [B]_{aq}$, equation 12 becomes:

$$\log J_{AB} = 2\log[A]_{aq} + \log\left(\frac{K_{11mem} D_A D_B \mathscr{D}_{AB} A}{L}\right) \quad \text{(Equation 13)}$$

Since the permeability of the ion-pair, $P_{app\,AB} = J_{AB} / [B]_{aq}\, A$, Equation 12 can be re-written to express the $P_{app\,AB}$ dependence on $[A]_{aq}$:

$$\log P_{app\,AB} = \log[A]_{aq} + \log\left(\frac{K_{11mem} D_A D_B \mathscr{D}_{AB}}{L}\right) \quad \text{(Equation 14)}$$

Thus, a log-log plot of J or P_{app} versus counterion concentration should give a slope of 1 as per Equation 12 and 14. Likewise, when $[A]_{aq} = [B]_{aq}$, a log-log plot of J versus counterion concentration should give a slope of 2 as per Equation 13. Equations 12–13 are similar in form to those previously derived by Duffey *et. al* describing the flux of tetrabuytlammonium nitrate through liquid membranes of n-heptyl cyanide.[19]

Experimental Section

Materials

1-hydroxy-2-naphthoic acid, trifluoroacetic acid, anhydrous dimethyl formamide (DMF), triethylamine, and 1-octanol were obtained from Sigma-Aldrich (St. Louis, MO). Oseltamivir phosphate was obtained from Sequoia Research Products Ltd (Pangbourne, UK). Acetylneuraminic acid (sialic acid) for zanamivir synthesis was purchased from TCI America Ltd (Portland, OR). All compounds were of the highest available quality and were used as received.

Guanidino Oseltamivir Synthesis

Guanidino oseltamivir was synthesized as shown in Scheme 1.[20] Briefly, oseltamivir was first converted to its guanidino analogue which was later deprotected to give guanidino oseltamivir as trifloroacetate salt. The synthetic procedure is given as follows:

(3R,4R,5S)-ethyl-4-acetamido-5-(2,3-bis(tert-butoxycarbonyl)guanidino)-3-(pentan-3-yloxy)cyclohex-1-enecarboxylate (2)—To a stirring solution of oseltamivir phosphate, **1**, (1g, 2.4 mmol), bis-boc thiourea (1.06g, 3.6 mmol) and triethyl amine (TEA, 1.1ml, 8 mmol) in 20ml DMF, was added Mercury (II) chloride (0.728g, 2.6 mmol) while stirring at 0 °C. The reaction was followed by thin layer chromatography (TLC) using ethylacetate:hexane (1:3). After approximately 1 hour, when all starting material was reacted, the reaction mixture was diluted with ethyl acetate and filtered. It was then washed with water and brine and dried over anhydrous magnesium sulfate. Column chromatography using hexane:ethyl acetate (10:1) gave pure intermediate, **2**, which is the precursor to guanidine oseltamivir, as white powder, in 89% overall yield. [^{1}H] NMR ($CdCl_3$, 500MHz) δ (ppm) 0.84–0.92 (m, 6H),1.23–1.30 (m, 3H), 1.49–1.55 (m, 22H), 1.91

(s, 3H), 2.37 (dd, 1H, *J* = 2.55, 2.55 Hz), 5.35 (dd, 1H, *J* = 5.35, 5.35 Hz), 3.34 (t, 1H, *J* = 5.65 Hz), 4.01–4.09 (m, 1H), 4.12–4.14 (m, 1H), 4.16–4.23 (m, 2H), 4.35–4.37 (m, 1H), 6.21 (d, 1H, *J* = 8.95 Hz) 8.64 (d, 1H, NH, *J* = 8.05), 11.39 (s, 1H, NH) ; ESI^+-MS, m/z: 555.3 $(M+H)^+$

(3R,4R,5S)-ethyl-4-acetamido-5-guanidino-3-(pentan-3-yloxy)cyclohex-1-enecarboxylate (3)—Compound **2** was boc deprotected using trifloroacetic acid. It was then stirred with 40% trifloroacetic acid in dichloromethane for about two hours.[21] Following the completion of the reaction (TLC, ESI-MS), compound **3 (Gaunidino Oseltamivir)** was lyophilized for approximately 48 hours to give a white powder as amorphous 2-TFA salt. Yield was nearly 100%. Purity was greater than 95% by HPLC. [^{1}H] NMR (Cd_3OD, 500MHz) δ (ppm) 0.90–0.96 (m, 6H), 1.32 (t, *J* = 7.1 Hz, 3H), 1.50–1.58 (m, 4H), 2.01 (s, 3H), 2.38 (dd, 1H, *J* = 9.1, 17.65Hz), 2.85 (dd, 1H, J = 5.05, 17.45 Hz), 3.42–3.45 (m, 1H), 3.85–3.88 (m, 1H), 3.93 (t, 1H, *J* = 9.65), 4.20–4.27 (m, 3H), 6.86 (s, 1H), 8.25 (d, 1H, NH, *J* = 8.3 Hz); ESI^+-MS, m/z: 355.2 $(M+H)^+$

Zanamivir Heptyl Ester Synthesis

Zanamivir heptyl ester was synthesized as shown in Scheme 2. Boc-protected zanamivir **2** was synthesized from sialic acid **1** using synthetic methods previously reported.[21–23] The heptyl ester of Boc- zanamivir **3** was synthesized from Boc-zanamivir by first forming the cesium salt followed by reaction with 1-bromoheptane in N,N-dimethyl formamide.[24] The final compound **4** was obtained by deprotection of Boc in presence of 30% trifluroacetic acid in dichloromethane.

5-Acetamido-2,6-anhydro-4-(2,3-bis(tert-butoxycarbonyl)guanidino)-3,4,5-trideoxy-D-glycero-D-galcto-non-2-enonic acid (Boc-Zan) 2—^{1}H NMR (CD_3OD) δ (ppm) 5.6 (d, *J* = 2.0 Hz, 1H), 5.01 (dd, *J* = 9.6, 2.1 Hz, 1H), 4.25 (dd, *J* = 10.8, 1.1 Hz, 1H), 4.18 (dd, *J* = 10.6, 9.6 Hz, 1H), 3.89 (ddd, *J* = 9.4, 6.2, 2.7 Hz, 1H), 3.84 (dd, *J* = 11.3, 2.8 Hz, 1H), 3.67 (dd, *J* = 11.3, 5.8 Hz, 1H), 3.57(d, *J* = 9.3 Hz, 1H), 1.9 (s, 3H), 1.55 (s, 9H), 1.50 (s, 9H); ESI-MS: 533 $(M+H)^+$.

5-Acetamido-2,6-anhydro-4-(2,3-bis(tert-butoxycarbonyl)guanidino)-3,4,5-trideoxy-D-glycero-D-galcto-non-2-enonic acid heptyl ester 3—A solution of **2** (50 mg) in 2 mL ethanol:water (3:1) was made neutral with 10% cesium carbonate. The reaction mixture was concentrated under reduced pressure and was re-dissolved in water which was lyophilized for 48 hours to yield cesium salt of **2**. 25 mg of **2** was dissolved in N, N-dimethylformamide (2 mL) and to it 1-bromoheptane (17mg, 94.9 mmol) was added and the reaction was allowed to stir at room temperature for 20 hours. The reaction mixture was concentrated under reduced pressure. The crude reaction mixture was purified by flash column chromatography using chloroform: methanol (25:1) as eluent to obtain **3** as a colorless oil (21 mg, 72%). ^{1}H NMR ($CDCl_3$) δ (ppm) 5.8(d, *J* = 2.0 Hz, 1H), 5.1(m, 1H), 4.2(m, 2H), 4.15 (m, 2H), 3.9(m, 1H), 3.8(m, 1H) 3.45(m, 2H), 2.01(s, 3H), 1.88(m, 2H), 1.52 (s, 9H), 1.50 (s, 9H), 1.3–1.5(m, 8H), 0.9(m, 3H); ESI-MS: 631 $(M+ H)^+$.

5-Acetamido-2,6-anhydro-4-(guanidino)-3,4,5-trideoxy-D-glycero-D-galcto-non-2-enonic acid heptyl ester 4—To 20 mg **4** 30% trifluroacetic acid in dichloromethane (2mL) was added and the reaction was stirred at room temperature for one hour. The progression of the reaction was monitored by TLC. The reaction mixture was concentrated in vacuo. The concentrate was dissolved in water and lyophilized for 48 hours to yield the final compound as a white fluffy solid (18 mg, 82%) ^{1}H NMR (CD_3OD) δ (ppm) 5.9 (d, *J* = 2.0 Hz, 1H), 5.5(m, 1H) 4.22 (m, 2H) 4.07(m, 2H), 3.85 (m, 1H), 3.70(m,

1H), 3.5 (m, 2H), 2.03(s, 3H), 1.7(m, 2H), 1.38–1.56 (m, 8H), 0.9(m, 3H) ; ESI-MS: 431.3 $(M+H)^+$.

High Performance Liquid Chromatography (HPLC)

HPLC experiments were performed on an Agilent Technologies (Palo Alto, CA) HPLC 1100 equipped with photodiode array detector and ChemStation for LC 3D software. Zanamivir heptyl ester was assayed using a 150mm × 4.6mm Agilent (Palo Alto, CA) XDB-C_{18} column with 5 μm particle size. The detection wavelength was 242 nm. The mobile phase consisted of 65:35 (v:v) 0.1% trifluoroacetic acid in water: acetonitrile and was pumped at a flow rate of 1.0 ml/min. Guanidino oseltamivir was assayed using a 150mm × 4.6mm Zorbax (Aston, PA) SB-C_{18} column with 5 μm particle size. The detection wavelength was 210 nm. The mobile phase consisted of 65:35 (v:v) 0.1% heptafluorobutyric acid in water: acetonitrile and was pumped at a flow rate of 1.0 ml/min. Injection volumes for all HPLC analyses ranged from 5 to 100 μL.

Octanol-Buffer (pH 6.5) Partitioning Experiments

Octanol-buffer (pH 6.5) partitioning studies were performed using a method described previously.[13] Solutions of each drug (50 μg/mL) were prepared in octanol saturated sodium phosphate buffer (50 mM, pH 6.5) with a molar excess of HNAP. These aqueous solutions were then equilibrated at 37 °C with an equivalent volume (0.5 mL) of buffer saturated octanol using magnetic stirring at 700 rpm for 24–36 hours. Three replicates of each determination were carried out to assess reproducibility. The octanol and aqueous phases were then separated by centrifugation. The total drug concentration in the aqueous phase, $[B_t]_{aq}$, was then determined by HPLC and the total drug concentration in the octanol phase, $[B_t]_{oct}$, was obtained by mass balance (i.e. $[B_t]_{oct}$ = total drug put into system − $[B_t]_{aq}$). From these data, the apparent octanol/buffer (pH 6.5) distribution coefficient, $D_B = [B_t]_{oct} / [B_t]_{aq}$, is determined

Caco-2 Cell Monolayer Assay—Caco-2 cells (passage 22–25) from American Type Culture Collection (Rockville, MD) were routinely maintained in Dulbecco's modified Eagle's medium (DMEM, Invitrogen Corp., Carlsbad, CA) containing 10% fetal bovine serum, 1% nonessential amino acids, 1 mM sodium pyruvate, and 1% L-glutamine. Cells were grown in an atmosphere of 5% CO_2 and 90% relative humidity at 37°C. The DMEM medium was replaced by fresh medium every three days. Cells were passaged upon reaching approximately 80% confluence using 4 ml trypsin-EDTA (Invitrogen Corp., Carlsbad, CA).

Transepithelial transport studies were performed using a method described previously with minor modifications.[13,25] Briefly, 8×10^4 cells/cm^2 were seeded onto collagen-coated membranes (12-well Transwell plate, 0.4-μm pore size, 12 mm diameter, Corning Costar, Cambridge, MA) and were allowed to grow for 21 days in order to obtain differentiated monolayers. TEER measurements were performed on the monolayers before and after the experiments (Millicell-ERS epithelial Voltohmmeter, Millipore Co., Bedford, MA). Monolayers with TEER values >300 Ωcm^2 were used for the study. On the day of the experiment, the DMEM was removed, and the monolayers were rinsed and incubated for 20 minutes with a blank transport buffer. The apical transport buffer contained 1 mM $CaCl_2$, 0.5 mM $MgCl_2{\cdot}6H_2O$, 145 mM NaCl, 3 mM KCl, 5 mM D-glucose, and 10 mM sodium phosphate buffer pH 6.5. The basolateral transport buffer was identical to the apical, except the 10 mM sodium phosphate buffer was pH 7.4. Following the 20 minute incubation, blank transport buffer was removed from the apical side and replaced by 0.5 ml of the drug solution in the uptake buffer (pH 6.5), with HNAP concentrations ranging from 0 to 24 mM. The basolateral side was loaded with 1.5 mL of pH 7.4 transport buffer. Throughout the experiment, the transport plates were kept in a shaking incubator (50 rpm) at 37°C. Samples

were taken from the receiver side at various time points up to 120 min (200 μL from basolateral side) and 200 μL of blank transport buffer was added following each sample withdrawal. At the last time point (120 min), sample was taken from the donor side as well, in order to confirm mass balance. Samples were immediately assayed for drug content by HPLC. TEER measurements were carried out after each transport study to assess Caco-2 monolayer confluence. Lucifer yellow permeability was determined in the presence of 0, 12, and 24 mM HNAP to assess the influence of counterion on Caco-2 monolayer integrity.

Permeability coefficients (P_{app}) across Caco-2 cell monolayers were calculated from the linear plot of drug accumulated in the receiver side versus time, using the following equation:

$$P_{app} = \frac{1}{C_0 A} \times \frac{dQ}{dt} \quad \text{(Equation 15)}$$

where dQ/dt is the steady-state appearance rate of the drug on the receiver side, C_0 is the initial concentration of the drug in the donor side, and A is the monolayer growth surface area (1.12 cm^2). Linear regression was carried out to obtain the steady-state appearance rate of the drug on the receiver side.

Rat Jejunal Perfusion

All animal experiments were conducted using protocols approved by the University Committee of Use and Care of Animals (UCUCA), University of Michigan, and the animals were housed and handled according to the University of Michigan Unit for Laboratory Animal Medicine guidelines. Male albino Wistar rats (Charles River, IN) weighing 250–280 g were used for all perfusion studies. Prior to each experiment, the rats were fasted overnight (12–18 h) with free access to water. Animals were randomly assigned to the different experimental groups.

The procedure for the *in-situ* single-pass intestinal perfusion followed previously published reports.[25–27] Briefly, rats were anesthetized with an intramuscular injection of 1 mL/kg of ketaminexylazine solution (9%:1%, respectively) and placed on a heated surface maintained at 37 °C (Harvard Apparatus Inc., Holliston, MA). The abdomen was opened by a midline incision of 3–4 cm. A proximal jejunal segment (3 ± 1 cm average distance of the inlet from the ligament of Treitz) of approximately 10 cm was carefully exposed and cannulated on two ends with flexible PVC tubing (2.29 mm i.d., inlet tube 40 cm, outlet tube 20 cm, Fisher Scientific Inc., Pittsburgh, PA). Care was taken to avoid disturbance of the circulatory system and the exposed segment was kept moist with 37 °C normal saline solution. Solutions of the test drug were prepared with HNAP at concentrations of 0–12 mM in the perfusate buffer. The perfusate buffer consisted of 1 mM $CaCl_2$, 0.5 mM $MgCl_2 \cdot 6H_2O$, 145 mM NaCl, 3 mM KCl, 5 mM D-glucose, and 10 mM sodium phosphate buffer pH 6.5 and 0.02 mg/mL of a non-absorbable marker. Phenol red was used as the non-absorbable marker for the perfusion studies using GO and zanamivir carboxylate was used as the non-absorbable marker for the studies using ZHE. All perfusate solutions were incubated in a 37 °C water bath and were pumped through the intestinal segment (Watson Marlow Pumps 323S, Watson-Marlow Bredel Inc., Wilmington, MA). The isolated segment was first rinsed with blank perfusion buffer, pH 6.5, at a flow rate of 0.5 mL/min in order to clean out any residual debris. At the start of the study, the test solutions were perfused through the intestinal segment at a flow rate of 0.2 mL/min. The perfusion buffer was first perfused for one hour, in order to ensure steady state conditions (as also assessed by the inlet over outlet concentration ratio of non-absorbable marker which approaches 1 at steady state). After reaching steady state, samples were taken in 10 min intervals for one hour (10, 20, 30, 40, 50, and 60 min). All samples, including perfusion samples at different time points, original

drug solution, and drug solution at the end of the experiment, were immediately assayed by HPLC. Following the termination of the experiment, the length of each perfused jejunal segment was accurately measured.

The net water flux in the single-pass rat jejunal perfusion studies, resulting from water absorption in the intestinal segment, was determined by measurement of the non-absorbable marker. The measured C_{out}/C_{in} ratio was corrected for water transport according to the following equation:

$$\frac{C'_{out}}{C'_{in}} = \frac{C_{out}}{C_{in}} \times \frac{C_{inref}}{C_{out\ ref}} \quad \text{(Equation 3.10)}$$

where C_{out} is the concentration of the test drug in the outlet sample, C_{in} is the concentration of the test drug in the inlet sample, $C_{in\ ref}$ is the concentration of non-absorbable marker in the inlet sample, and $C_{out\ ref}$ is the concentration of non-absorbable marker in the outlet sample. The effective permeability (P_{eff}) through the rat gut wall in the single-pass intestinal perfusion studies was determined assuming the "plug flow" model expressed in the following equation:[28]

$$P_{eff} = \frac{-Q \ln(C'_{out}/C'_{in})}{2\pi RL} \quad \text{(Equation 16)}$$

where Q is the perfusion buffer flow rate, C'_{out}/C'_{in} is the ratio of the outlet concentration and the inlet or starting concentration of the tested drug that has been adjusted for water transport via Equation 3.10, R is the radius of the intestinal segment (set to 0.2 cm), and L is the length of the intestinal segment.

Statistical Analysis

Values are expressed as the mean of at least 3 measurements, +/− the standard deviation (SD). Linear regression of the data using Equations 4 and 14 was carried out using SigmaPlot 2004 for Windows Version 9.01.

Results

Physical Chemical Properties of GO, ZHE, and HNAP

The physical and chemical properties of GO, ZHE, and HNAP are summarized in Table 1 and their chemical structures are shown in Figure 1. Both anti-viral agents possess a strongly basic guanidino functionality with cpKa of 12.80 for GO and 11.26 for ZHE. The inherent lipophilicities of GO and ZHE are similar as the compounds have nearly equivalent values of cLog P (0.83 vs. 0.69) and Log D (−1.17 vs. −1.31). HNAP possesses a carboxylic acid (pKa 2.70) which makes the compound anionic at pH 6.5 and the naphthalene functionality which imparts high lipophilicity (cLog P 3.29), making it an ideal lipophilic ion-pairing agent.

Octanol-Buffer (pH 6.5) Partitioning of the Ion-Pairs

The double reciprocal plots of the apparent octanol-buffer (pH 6.5) distribution coefficients of the drugs as a function of counterion concentration are shown in Figures 2–3 for the GO-HNAP and ZHE-HNAP ion-pairs. The double reciprocal plots for both ion-pair systems gave highly linear results ($R^2 > 0.99$), indicating excellent agreement with the quasi-equilibrium transport model (Equation 4). Table 2 summarizes the values of K_{11aq}, K_{11oct}, and Log P_{AB} for each ion-pair obtained via linear regression of the double reciprocal plots using Equation 4. Both ion-pairs showed substantially enhanced lipophilicity as compared to

the free drug. The GO-HNAP ion-pair (Log P_{AB} = 4.50) was over 2 orders of magnitude more lipophilic than the ZHE-HNAP ion-pair (Log P_{AB} = 1.89). Conversely, the K_{11aq} of ZHE-HNAP was over 2 orders of magnitude higher than the K_{11aq} of the GO-HNAP ion-pair (388 M^{-1} vs. 2.91 M^{-1}), indicating much stronger intermolecular complexation for the ZHE-HNAP ion-pair. The stronger aqueous binding constant for the ZHE-HNAP ion-pair results in a higher $\%[AB]_{aq}$ at a given HNAP concentration. For example at 10 mM HNAP concentration, $\%[AB]_{aq}$ is nearly 80% for the ZHE-HNAP ion-pair as compared to only 2.8% for the GO-HNAP ion-pair (Table 2). Values of K_{11oct} on the order of 10^5 M^{-1} were observed, indicating essentially 100% complexation in the octanol phase for both ion-pairs (Table 2).

Ion-pair Mediated Transport Across Caco-2 Cell Monolayers

The GO-HNAP and ZHE-HNAP ion-pairs were evaluated in the Caco-2 cell monolayer assay. In all of the experiments, the drug concentration was held constant and only the HNAP counterion concentration was increased, to clearly discern the effect of HNAP on Caco-2 cell monolayer integrity. The Caco-2 permeability of lucifer yellow in the presence of 0, 12, and 24 mM HNAP was also determined as a negative control. Lucifer yellow permeability was below the limit of quantitation ($<3\times10^{-7}$ cm/s) at all HNAP concentrations, indicating that an increase in drug permeability in the presence of HNAP is not due to an effect on membrane integrity. No significant change in TEER values was obtained before and after experiment at 0, 12, and 24 mM HNAP concentration, further indicating that HNAP did not disrupt membrane integrity.

Figure 4 shows the dependence of GO P_{app} on HNAP concentration (0, 12, 18, and 24 mM) in the Caco-2 cell mono-layer assay. GO P_{app} increased with counterion concentration, consistent with the ion-pair mediated transport mechanism. No detectable transport was observed for GO in the absence of HNAP, whereas substantial permeability was observed for GO at HNAP concentrations of 12, 18, and 24 mM (Figure 4). A linear relationship with a slope near 1 was obtained from the log-log plot of GO P_{app} versus HNAP concentration (Figure 4 inset). This relationship is consistent with the quasi-equilibrium ion-pair mediated transport model expressed in Equation 14.

Figure 5 shows the dependence of ZHE P_{app} on HNAP concentration (0, 6, 12, and 24 mM) in the Caco-2 cell monolayer assay. ZHE P_{app} also increased with HNAP concentration, consistent with an ion-pair transport mechanism. No detectable transport was observed for ZHE in the absence of HNAP, whereas substantial permeability was observed for ZHE at HNAP concentrations of 6, 12, and 24 mM (Figure 5). As observed for the GO-HNAP ion-pair, a linear relationship with a slope near 1 was obtained from a log-log plot of ZHE P_{app} versus HNAP concentration (Figure 5 inset). This relationship is consistent with the quasi-equilibrium ion-pair mediated transport model expressed in Equation 14.

Ion-pair Mediated Transport Across Rat Jejunum

The ability of HNAP to facilitate the intestinal permeation of GO and ZHE via ion-pair formation was evaluated in the rat jejunal perfusion assay. Figure 6 shows the P_{eff} of GO perfused across rat jejunal segments alone and also in the presence of 12 mM HNAP. No effective permeability was observed for GO alone and co-perfusion of GO with 12 mM HNAP resulted in no significant increase in P_{eff} (Figure 6).

Figure 7 shows the dependence of ZHE P_{eff} on HNAP concentration in the rat jejunal perfusion assay. ZHE was perfused alone and also in the presence of 4 and 10 mM HNAP. Essentially zero P_{eff} was observed for ZHE in the absence of HNAP, whereas substantial increases in rat jejunal P_{eff} were observed for ZHE with increasing HNAP concentration

(Figure 7). Table 2 summarizes the K_{11aq}, Log P_{AB}, and rat jejunal P_{eff} values for the ZHE-HNAP and GO-HNAP ion-pairs.

Discussion

The enhancement of the intestinal membrane permeability of the highly polar anti-viral agents ZHE and GO via ion-pairing with the lipophilic counterion HNAP is described in this paper. No oral delivery route currently exists for zanamivir or GO. Therefore, enabling the oral absorption of these drugs via an ion-pairing approach is a very significant advance, with practical implications. In addition to providing a novel approach to enable the oral delivery of these highly polar anti-viral agents, this work also provides new insights into the underlying mechanisms and key attributes that govern the success or failure of the ion-pairing strategy to increase oral absorption.

Absorption enhancement using ion-pairs has been the topic of much discussion and debate in the literature.[30–35] There are reports of significant increases in membrane transport using ion-pairs[13, 36–41] However, only a few of the studies have been successful in significantly increasing intestinal absorption *in-vivo*. This is largely because the mechanism by which ion-pairs may increase oral absorption, including the important parameters and key attributes that determine success or failure of a given ion-pair, are not well understood. Moreover, mathematical models describing ion-pair mediated membrane transport remain under utilized.

An ion-pairing approach for increasing oral absorption has several advantages. The approach is simple in principle and eliminates the need for prodrug uptake by transporters and activation by specific enzymes. The ion-pair in solution may be absorbed and then readily dissociate after absorption via dilution in the bloodstream. Moreover, the approach does not rely on disrupting membrane integrity to facilitate absorption. A potential disadvantage of the ion-pairing approach is that the ionic bonding and other non-covalent interactions (i.e hydrogen bonding) may be too weak in solution to facilitate membrane permeation.

The chemical structures and physical chemical properties of ZHE, GO, and HNAP are shown in Figure 1 and Table 1. Zanamivir carboxylate is highly polar (clogP = −3.63), however, the heptyl ester provides significantly improved lipophilicity (clogP = 0.69). Zanamivir also possesses a highly basic guanidinium functionality (cpK_a = 11.26) and elimination of the carboxylate through formation of the heptyl ester makes the compound positively charged over the entire physiologically relevant pH range (Figure 1). Thus, addition of the heptyl ester makes zanamivir amenable to permeability enhancement via ion-pairing in two important ways 1) esterfication imparts the positive charge needed for ion-pair formation and 2) addition of a lipophilic (e.g. heptyl) ester imparts enough inherent lipophilicity to zanamivr that may be further enhanced via ion-paring with a lipophilic counterion.

GO is the guanidino analog of oseltamivir. GO has a guanido functionality off the 5 position of the core cyclohexene ring instead of a primary amine, as in the case of oseltamivir (Figure 1). The clog P of GO is 0.83 (Table 1), which indicates that the unionized form of the molecule is moderately lipophillic. However, GO possesses a highly basic guanidinium functionality (cpK_a=12.8) which makes the compound positively charged over the entire physiologically relevant pH range (Figure 1). This highly charged nature of GO gives rise to a low clog D of −1.17 at pH 7 (Table 1), which leads to very poor permeability and low fraction absorbed dose absorbed after oral administration.[12] However, these properties also

make GO an ideal candidate for permeability enhancement via ion-pair formation with lipophillic acids.

The inherent lipophilicity of HNAP (cLog P = 3.29) and relatively strong acidity (pK_a = 2.70) makes it an ideal ion-pairing agent for increasing the lipophilicity of highly polar molecules such as ZHE and GO.[13] Indeed, the lipophilicity of both GO and ZHE were substantially enhanced via ion-pairing with HNAP. As compared to the free drug, HNAP increased the log P of GO by 3.7 units and the log P of ZHE by 1.2 units (Tables 1–2). Interestingly, the GO-HNAP ion-pair was over 2 orders of magnitude more lipophilic than the ZHE-HNAP ion-pair (Table 2), indicating the HNAP was more effective in increasing the lipophilicity of GO as compared to ZHE. Conversely, the aqueous phase binding constant of the ZHE-HNAP ion-pair was markedly stronger than that of the GO-HNAP ion-pair (388 M^{-1} vs. 2.91 M^{-1}), indicating much stronger intermolecular complexation for the ZHE-HNAP ion-pair (Table 2). The magnitude of the binding constant reflects the strength of the interaction between the acid and base components of the ion-pair. The tightness of the ion-pair binding is governed primarily by the strength of the ionic bond. The difference in pK_a between the acid and base of the ion-pair (ΔcpK_a) should reflect the relative strength of the ionic bond of the ion-pair. As shown in Table 1, the guanidino cpK_a for ZHE is 1.5 log units lower than the cpK_a for GO. Therefore, the much stronger K_{11aq} for ZHE-HNAP as compared to GO-HNAP cannot be explained by the relative strength of the ionic bonds (i.e. ΔcpK_a between drug and HNAP). So other non-ionic interactions, namely hydrogen bonding, must also contribute to the overall strength of the ion-pair interaction. The number of hydrogen bond donor (HBD) and hydrogen bond acceptor (HBA) moieties in the acidic and basic components should reflect the relative number and strength of hydrogen bonds in the ion-pair. Indeed, ZHE contains a significantly higher number of HBD and HBA moieties as compared to GO (HBD + HBA = 20 vs. 13), suggesting that the markedly stronger K_{11aq} for ZHE-HNAP compared to GO-HNAP must be primarily due to the increased number and strength of the hydrogen bonds within the complex.

The ability of HNAP to enhance the P_{app} of GO and ZHE was evaluated in the Caco-2 cell monolayer assay. The permeability for both GO and ZHE increased in the presence of HNAP in a concentration dependent manner, whereas no detectable transport was observed in the absence of counterion for either compound (Figures 4–5). As predicted from a quasi-equilibrium analysis of ion-pair mediated membrane transport, an order of magnitude increase in Caco-2 cell monolayer permeability was observed per log increase in HNAP concentration for GO and ZHE. As such, log-log plots of apparent permeability versus HNAP concentration gave linear relationships with slope near 1 (Figures 4–5), thus supporting an ion-pair mediated transport mechanism.

The ability of HNAP to facilitate the intestinal permeation of GO and ZHE via ion-pair formation was evaluated in the rat jejunal perfusion assay. Essentially zero P_{eff} was observed for both GO and ZHE in the absence of the HNAP counterion (Figures 6–7). This is consistent with the very low F < 0.04 that has been reported in rat for both GO and zanamivir[12], as well as the non-detectable P_{app} observed in the Caco-2 assay for these compounds (Figures 4–5). Co-perfusion of GO with 12 mM HNAP resulted in no significant increase in P_{eff} (Figure 6). However, HNAP substantially increased the rat jejunal P_{eff} for ZHE in a concentration dependent manner, to 2.1×10^{-5} cm/s at 4 mM HNAP and 4.0×10^{-5} cm/s at 10 mM HNAP (Figure 7). In fact, the rat jejunal P_{eff} of ZHE in the presence of 4 and 10 mM HNAP was comparable to that of metoprolol (3.3×10^{-5} cm/s), which is generally recognized as the standard for the low-high permeability boundary.[28, 42] This is a very significant result with practical implications, since no oral delivery route currently exists for zanamivir.

ZHE was more successful than GO in the rat jejunal perfusion assay despite the fact that the ZHE-HNAP ion-pair is significantly less lipophilic than the GO-HNAP ion pairs (Table 3). Therefore, the enhancement of ZHE rat jejunal P_{eff} by ion-pairing with HNAP may be attributed to the considerably higher value of K_{11aq} = 388 M^{-1} as compared to the GO-HNAP ion-pair K_{11aq} = 2.91 M^{-1} (Table 3). The much higher binding constant of the ZHE-HNAP the ion-pair makes it much more resistant to ion-exchange with competing endogenous anions. In the rat jejunum, there are endogenous anions present such as sialic acid, bile acids, phosphatidylserine, and phosphatidylinositol which may compete with HNAP for binding with the cationic drug. It is interesting to note that HNAP failed to increase the permeability GO across rat jejunum (Figure 6), yet successfully increased the permeability of GO across Caco-2 cell monolayers (Figure 4). One possible explanation for this observation is that Caco-2 cell monolayers lack the mucin layer that is present at the membrane-aqueous interface *in-vivo*.[43–44] The ion-pairs may be particularly susceptible to dissociation and ion-exchange within the mucin layer at the membrane-aqueous interface, where the presence of sialic acid creates a barrier of negative charge at the surface of the membrane. The relatively weak binding constant of the GO-HNAP ion-pair makes it more likely to dissociate at the membrane-aqueous interface in rat jejunum, however GO-HNAP may remain intact during permeation across Caco-2 cell monolayers since the mucin layer is not present. Conversely, the much higher binding constant for the ZHE-HNAP ion-pair makes it more likely to remain intact during the entire membrane permeation process in both rat jejunum and Caco-2 cell monolayers..

Conclusions

In conclusion, we were able to overcome intestinal permeability barriers for the highly polar antiviral agents ZHE and GO, which is the critical step towards successful oral administration of these important drugs. Several key attributes for successful ion-pair mediated membrane transport, were apparent from this work. Successful ion-pair mediated membrane transport was observed in the Caco-2 monolayer assay when the ion-pair Log P_{AB} values were in the range of approximately 2–5. In addition to sufficient lipophilicity of the ion-pair, a strong K_{11aq} value is required to prevent dissociation and ion-exchange with competing endogenous ions (e.g. phosphatidylserine, phosphatidylinositol, sialic acid, bile acids) such that the ion-pair will remain intact during the entire membrane permeation process. The ZHE-HNAP ion-pair, with binding constant on the order of 100 to 1000 M^{-1}, enabled successful ion-pair mediated membrane transport in the rat jejunal perfusion assay, whereas the GO-HNAP ion-pair, with binding constants on the order of 1 to 10 M^{-1}, was not successful. Overall, this work provides novel insights and quantitative understanding of the underlying mechanisms governing the success or failure of the ion-pairing strategy to increase oral absorption. This increased understanding enables the more efficient and intelligent design of drug delivery systems which utilize ion-pairing to improve intestinal membrane permeation and oral absorption.

References

1. Kasim NA, Whitehouse M, Ramachandran C, Bermejo M, Lennernäs H, Hussain AS, Junginger HE, Stavchansky SA, Midha KK, Shah VP, Amidon GL. Molecular Properties of WHO Essential Drugs and Provisional Biopharmaceutical Classification. Mol. Pharmaceutics. 2004; 1:85–96.
2. Takagi T, Ramachandran C, Bermejo M, Yamashita S, Yu LX, Amidon GL. A Provisional Biopharmaceutical Classification of the Top 200 Oral Drug Products in the United States, Great Britain, Spain, and Japan. Mol. Pharmaceutics. 2006; 3:631–643.
3. Dahan A, Miller JM, Amidon GL. Prediction of Solubility and Permeability Class Membership: Provisional BCS Classification of the World's Top Oral Drugs. AAPS J. 2009; 11:740–746. [PubMed: 19876745]

4. Lipinski CA. Drug-Like Properties and the Causes of Poor Solubility and Poor Permeability. J. Pharmacol. Toxicol. Meth. 2001; 44:235–249.
5. Martinez MN, Amidon GL. A Mechanistic Approach to Understanding the Factors Affecting Drug Absorption: A Review of Fundamentals. Pharmacokin. and Pharmacodyn. 2002; 42:620–643.
6. Lipka E, Crison J, Amidon GL. Transmembrane Transport of Peptide Type Compounds: Prospects for Oral Delivery. J. Con. Rel. 1996; 39:121–129.
7. Walter E, Kissel T, Amidon GL. The Intestinal Peptide Carrier: A Potential System for Small Peptide Derived Drugs. Adv. Drug Del. Rev. 1996; 20:33–58.
8. Amidon GL, Han H, Oh DM, Walter E, Hilfinger JM. Oral Administration of Peptide and Protein Drugs. Alfred Benzon. Symposium. 1998; 43:146–156.
9. Shin H, Landowski CP, Sun D, Amidon GL. Transporters in the GI Tract. Meth. Prin. Med. Chem. 2003; 18:245–287.
10. von Itzstein M. The War Against Influenza: Discovery and Development of Sialidase Inhibitors. Nat. Rev. Drug Disc. 2007; 6:967–974.
11. Massingale S, et al. Emergence of a Novel Swine-Origin Influenza A (H1N1) Virus in Humans. New England J Med. 2009; 360:2605–2615. [PubMed: 19423869]
12. Li W, Escarpe PA, Eisenberg EJ, Cundy KC, Sweet C, Jakeman KJ, Merson J, Lew W, Williams M, Zhang L, Kim CU, Bischofberger N, Chen MS, Mendel DB. Identification of GS 4104 as an Orally Bioavailable Prodrug of the Influenza Virus Neuraminidase Inhibitor GS 4071. Antimicrob. Agents Chemo. 1998; 42:647–653.
13. Miller JM, Dahan A, Gupta D, Varghese S, Amidon GL. Quasi-Equilibrium Analysis of the Ion-Pair Mediated Membrane Transport of Low-Permeability Drugs. J. Con. Rel. 2009; 137:31–37.
14. Miller, JM. PhD Thesis. Ann Arbor: University of Michigan; 2009. The Impact of Molecular Complexation on Intestinal Membrane Permeability.
15. Connors, KA. Binding Constants. The Measurement of Molecular Complex Stability. New York: John Wiley & Sons; 1987.
16. Grant, DJW.; Higuchi, T. Ion Pairs and Solubility Behavior. In: Weissberger, A., editor. Solubility Behavior of Organic Compounds. New York: John Wiley & Sons; 1990. p. 399-433.
17. Higuchi T. Physical Chemical Analysis of Percutaneous Absorption Process from Creams and Ointments. J. Soc. Cosmet. Chem. 1960; 11:85–97.
18. Higuchi, T. Prodrug, Molecular Structure and Percutaneous Delivery. In: Roche, EB., editor. Design of Biopharm Properties Through Prodrugs and Analogs. Washington D.C.: American Pharmaceutical Association Academy of Pharmaceutical Sciences; 1977. p. 409-421.
19. Duffey ME, Evans DF, Cussler EL. Simultaneous Diffusion of Ions and Ion Pairs Across Liquid Membranes. J. Mem. Sci. 1978; 3:1–14.
20. Shitara E, Nishimura Y, Nerome K, Hiramoto Y, Takeuchi T. Synthesis of 6-Acetamido-5-Amino- and -5-Guanidino-3, 4-Dehydro-N-(2-Ethylbutyryl)- 3-Piperidinecarboxylic Acids Related to Zanamivir and Oseltamivir, Inhibitors of Influenza Virus Neuraminidases. Org. Lett. 2000; 2:3837–3840. [PubMed: 11101432]
21. Masuda T, Yoshida S, Arai M, Kaneko S, Yamashita M, Honda T. Synthesis and Anti-Influenza Evaluation of Polyvalent Sialidase Inhibitors Bearing 4-Guanidino-Neu5Ac2en Derivatives. Chem. Pharm. Bull. Tokyo. 2003; 51:1386–1398. [PubMed: 14646315]
22. Chandler M, Bamford MJ, Conroy R, Lamont B, Patel B, Patel VK, Steeples IP, Storer R, Weir NG, Wright M, Williamson C. Synthesis of the Potent Influenza Neuraminidase Inhibitor 4-Guanidino Neu5Ac2en. X-Ray Molecular Structure of 5-Acetamido-4-Amino-2,6-Anhydro-3,4,5-Trideoxy-D-Erythro-L-Gluco-Nonionic Acid. J. Chem. Soc. Perk. Trans. 1. 1995; 9:1173–1180.
23. Martin R, Witte KL, Wong CH. The Synthesis and Enzymatic Incorporation of Sialic Acid Derivatives for Use as Tools to Study the Structure, Activity, and Inhibition of Glycoproteins and Other Glycoconjugates. Bioorg Med Chem. 1998; 6:1283–1292. [PubMed: 9784869]
24. Ogura H, Furuhata K, Sato S, Anazawa K, Itoh M, Shitori Y. Synthesis of 9-O-Acyl- And 4-O-Acetyl-Sialic Acids. Carbohydr. Res. 1987; 167:77–86. [PubMed: 3690578]
25. Dahan A, Amidon GL. Segmental Dependent Transport of Low Permeability Compounds Along the Small Intestine Due to P-Glycoprotein: The Role of Efflux Transport in the Oral Absorption of BCS Class III Drugs. Mol. Pharmaceutics. 2009; 6:19–28.

26. Kim JS, Mitchell S, Kijek P, Tsume Y, Hilfinger J, Amidon GL. The Suitability of an In-Situ Perfusion Model for Permeability Determinations: Utility for BCS Class I Biowaiver Requests. Mol. Pharmaceutics. 2006; 3:686–694.
27. Dahan A, Sabit H, Amidon GL. Multiple Efflux Pumps are Involved in the Transepithelial Transport of Colchicine: Combined Effect of P-Glycoprotein and Multidrug Resistance-Associated Protein 2 Leads to Decreased Intestinal Absorption Throughout the Entire Small Intestine. Drug Met. Disp. 2009; 37:2028–2036.
28. Fagerholm U, Johansson M, Lennernas H. Comparison Between Permeability Coefficients in Rat and Human Jejunum. Pharm. Res. 1996; 13:1336–1342. [PubMed: 8893271]
29. Stahl, PH.; Wermuth, CG. Monographs on Acids and Bases. In: Stahl, PH.; Wermuth, CG., editors. Handbook of Pharmaceutical Salts Properties, Selection, and Use. Zürich: Verlag Helvetica Chimica Acta; 2002. p. 265-327.
30. Tomlinson E. Never Mix a Cation with an Anion? Pharm. Int. 1980; 8:156–158.
31. Jonkman JHG, Hunt CA. Ion Pair Absorption of Ionized Drugs- Fact or Fiction? Pharm. Weekblad Sci. Ed. 1983; 5:41–48.
32. Neubert R. Ion Pair Transport Across Membranes. Pharm. Res. 1989; 6:743–747. [PubMed: 2682590]
33. Quintanar-Guerrero D, Allémann E, Fessi F, Doelker E. Applications of the Ion-Pair Concept to Hydrophilic Substances with Special Emphasis on Peptides. Pharm. Res. 1997; 14:119–127. [PubMed: 9090697]
34. Meyer JD, Manning MC. Hydrophobic Ion Pairing: Altering the Solubility Properties of Biomolecules. Pharm. Res. 1998; 15:188–193. [PubMed: 9523302]
35. Lengsfeld CS, Pitera D, Manning M, Randolph TW. Dissolution and Partitioning Behavior of Hydrophobic Ion-Paired Compounds. Pharm. Res. 2002; 19:1572–1576. [PubMed: 12425478]
36. Irwin GM, Kostenbauder HB, Dittert LW, Staples R, Misher A, Swintosky JV. Enhancement of Gastrointestinal Absorption of a Quaternary Ammonium Compound by Trichloroacetate. J. Pharm. Sci. 1969; 58:313–315. [PubMed: 4388699]
37. Gibaldi M, Grundhofer B. Enhancement of Intestinal Absorption of a Quaternary Ammonium Compound by Salicylate and Trichloroacetate. J. Pharm. Sci. 1973; 62:343–344. [PubMed: 4686423]
38. Walkling WD, Holmes DG, Cressman WA, Dix RK, Piperno E, Mosher AH. Possible Ion-Pair Mediated Absorption of Mixidine II: Plasma Levels and Histology. J. Pharm. Sci. 1978; 67:948–950. [PubMed: 26792]
39. Dal Pozzo A, Acquasaliente M, Geron MR. New Heparin Complexes Active By Intestinal Absorption: I-Multiple Ion Pairs With Basic Organic Compounds. Thromb. Res. 1989; 56:119–124. [PubMed: 2595670]
40. Ross BP, DeCruz SE, Lynch TB, Davis-Goff K, Toth I. Design, Synthesis, and Evaluation of a Liposaccharide Drug Delivery Agent: Application to the Gastrointestinal Absorption of Gentamicin. J. Med. Chem. 2004; 47:1251–1258. [PubMed: 14971905]
41. Mrestani Y, Härtl A, Neubert RHH. Influence of Absorption Enhancers on the Pharmacokinetic Properties of Non-Oral β-Lactam-Cefpirom Using the Rabbit (Chinchilla) *in Vivo* Model. Int. J. Pharm. 2006; 309:67–70. [PubMed: 16377108]
42. Lennernäs H. Intestinal Permeability and its Relevance for Absorption and Elimination. Xenobiotica. 2007; 37:1015–1051. [PubMed: 17968735]
43. Walter E, Janich S, Roessler BJ, Hilfinger JM, Amidon GL. HT29-MTX/Caco-2 Co-cultures as an in Vitro Model for the Intestinal Epithelium: In Vitro-in Vivo Correlation with Permeability Data from Rats and Humans. J. Pharm. Sci. 1996; 85:1070–1076. [PubMed: 8897273]
44. Pontier C, Pachot J, Botham R, Lenfant B, Arnaud P. HT29-MTX and Caco-2/TC7 Monolayers as Predictive Models for Human Intestinal Absorption: Role of the Mucus Layer. J. Pharm. Sci. 2001; 90:1608–1619. [PubMed: 11745719]

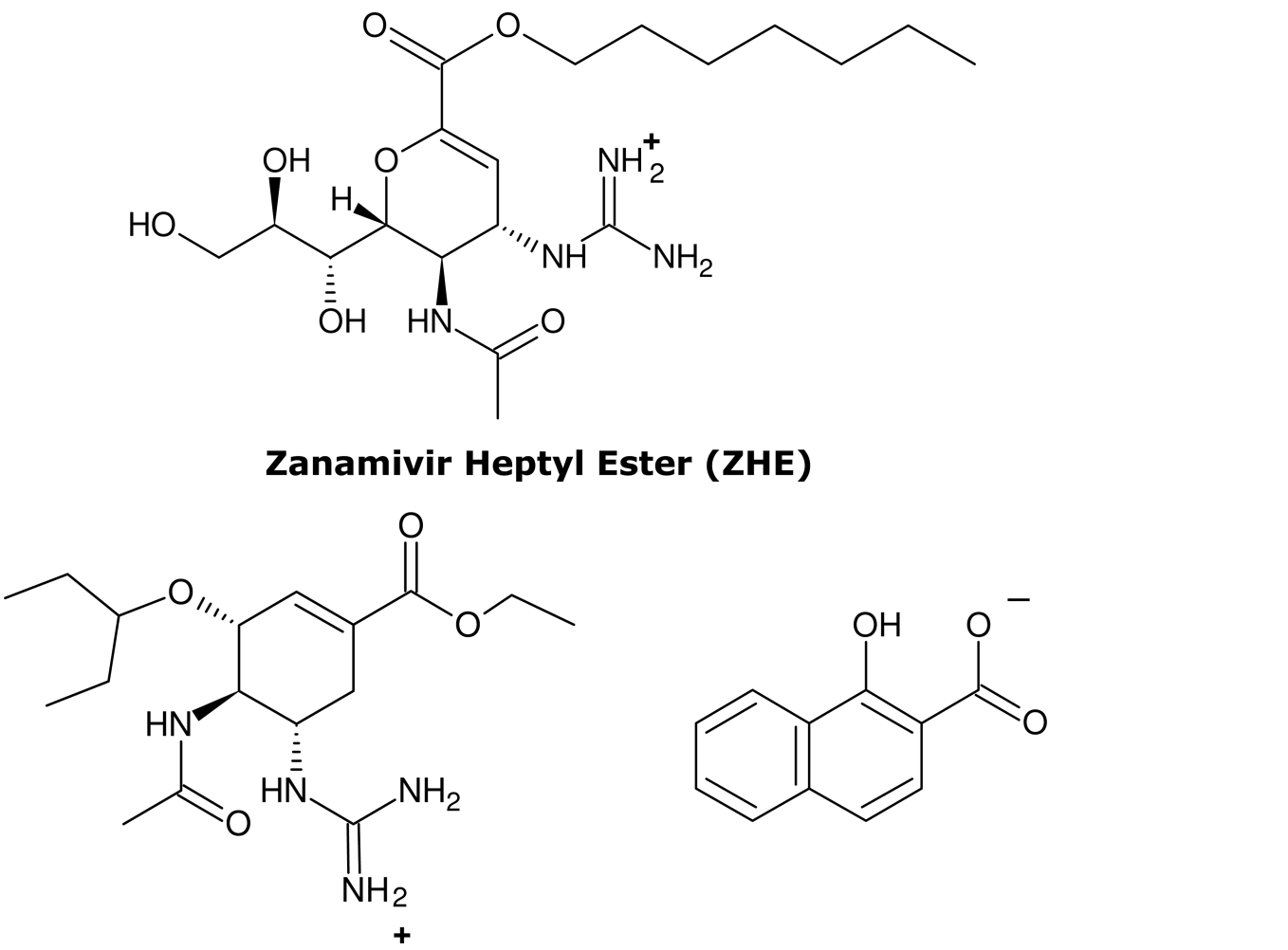

Figure 1.
Chemical structures of ZHE, GO, and HNAP. Ionization states at pH 6.5 as per pK_a values in Table 1 are shown for reference.

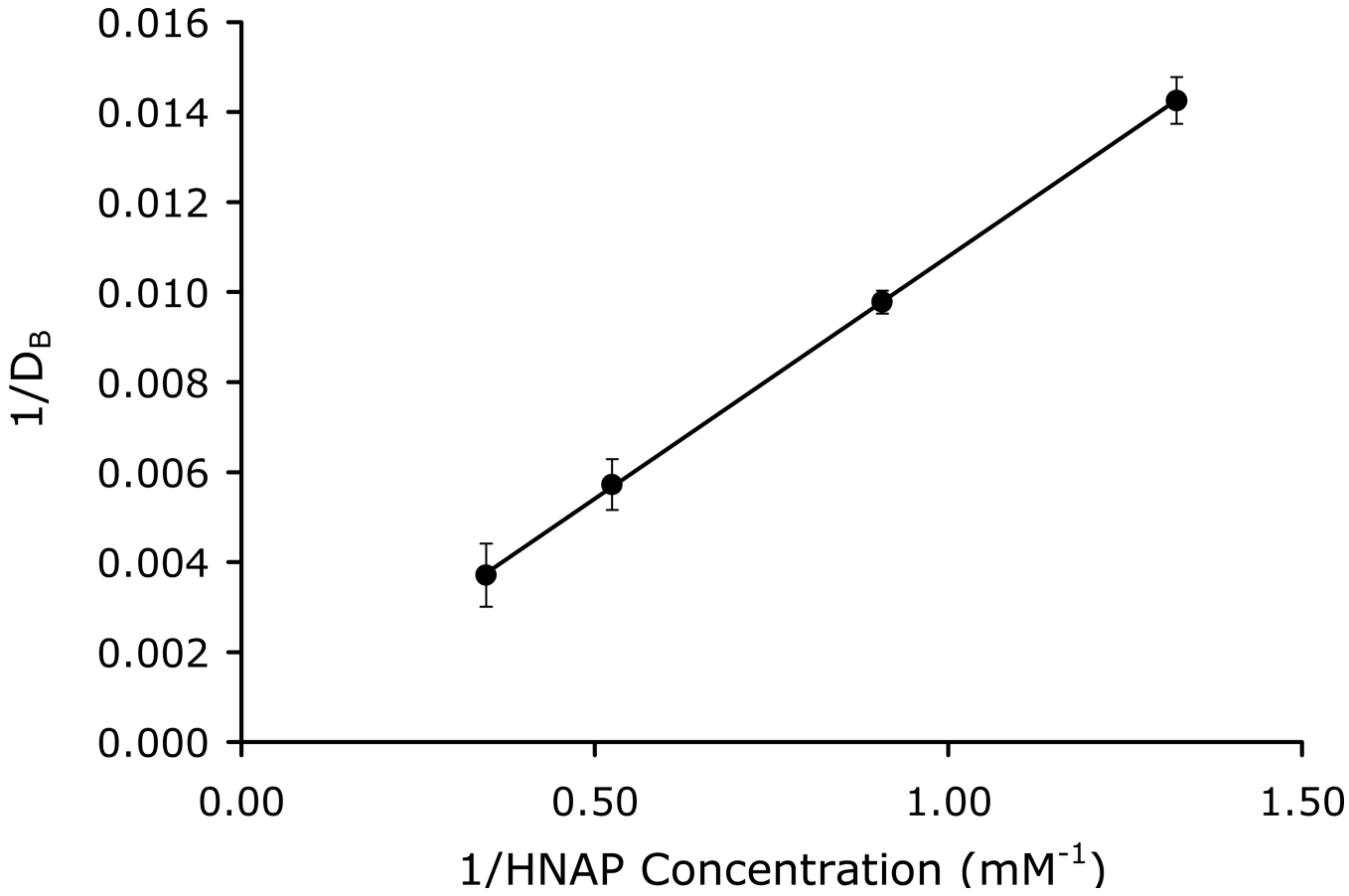

Figure 2.
Double reciprocal plot of the apparent octanol-buffer (pH 6.5) distribution coefficient of GO as a function of HNAP concentration.

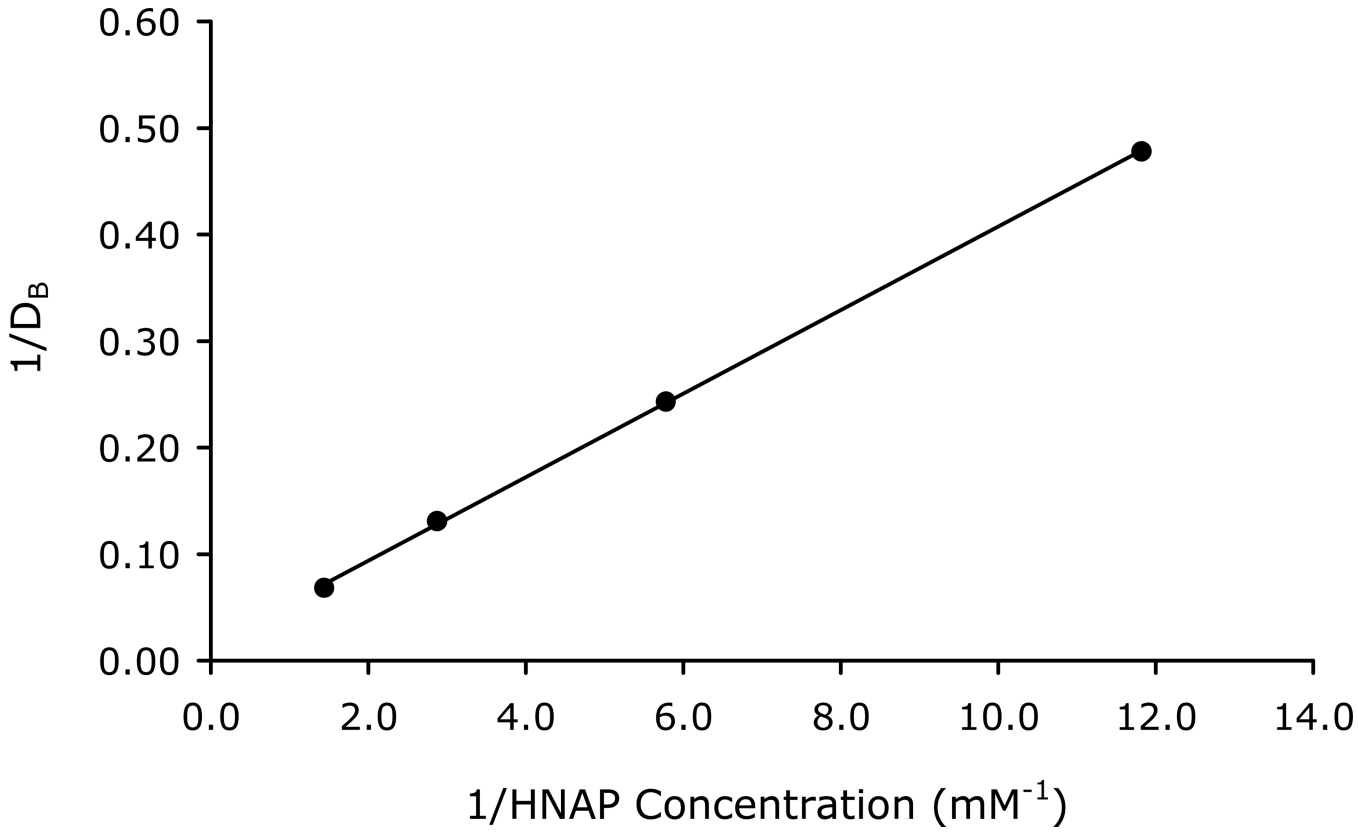

Figure 3.
Double reciprocal plot of the apparent octanol-buffer (pH 6.5) distribution coefficient of ZHE as a function of HNAP concentration.

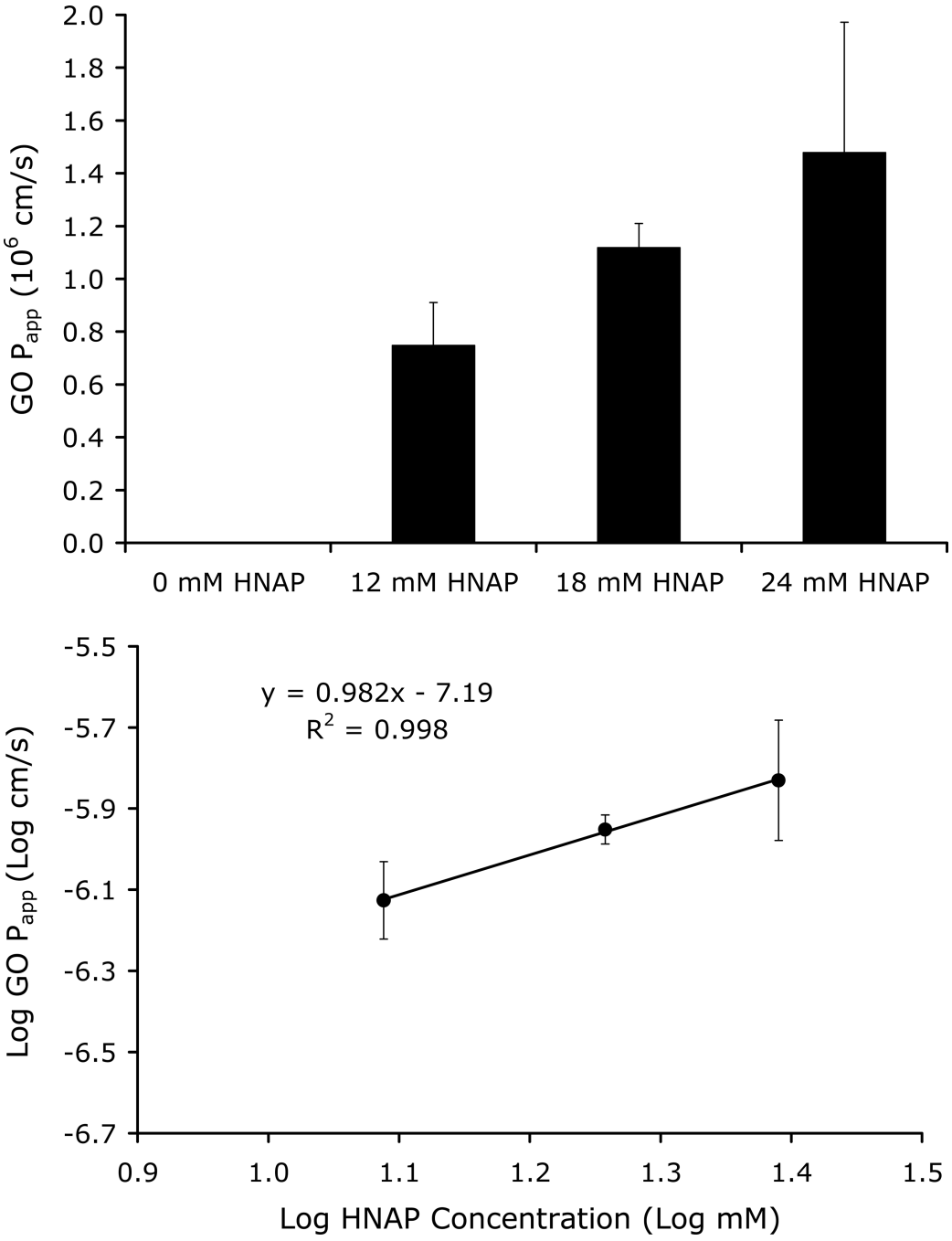

Figure 4.

Top: Dependence of GO P_{app} on HNAP concentration in Caco-2 cell assay. *Bottom:* Log GO P_{app} across Caco-2 cell monolayers as a function of Log HNAP concentration. Linear relationship with a slope near 1 is consistent with an ion-pair mediated transport mechanism as per Equation 14.

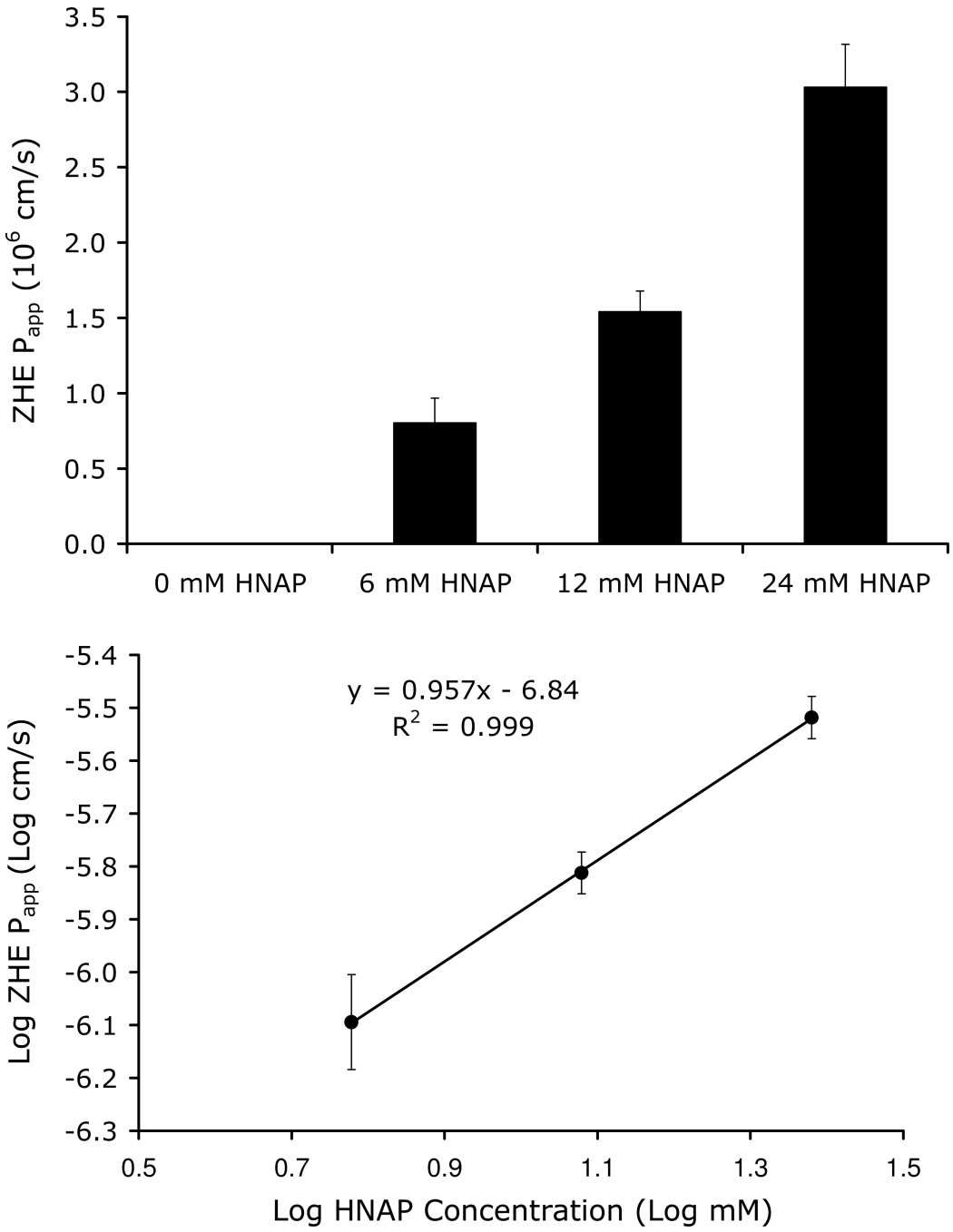

Figure 5.

Top: Dependence of ZHE P_{app} on HNAP concentration in Caco-2 cell assay

Bottom: Log ZHE P_{app} across Caco-2 cell monolayers as a function of Log HNAP concentration. Linear relationship with a slope near 1 is consistent with an ion-pair mediated transport mechanism as per Equation 14.

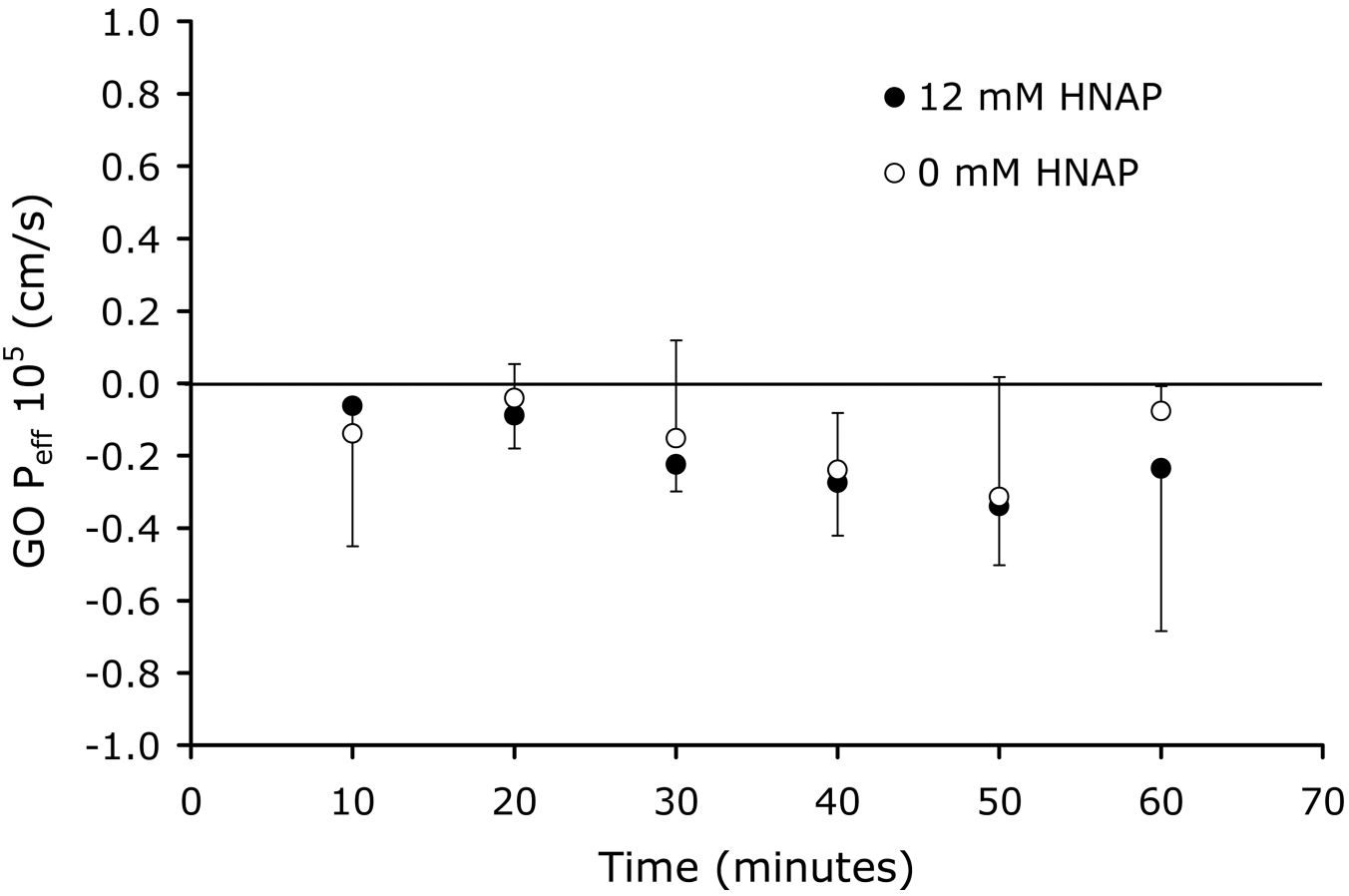

Figure 6.
GO P_{eff} versus time in rat jejunal perfusion assay at 0 mM and 12 mM HNAP concentrations

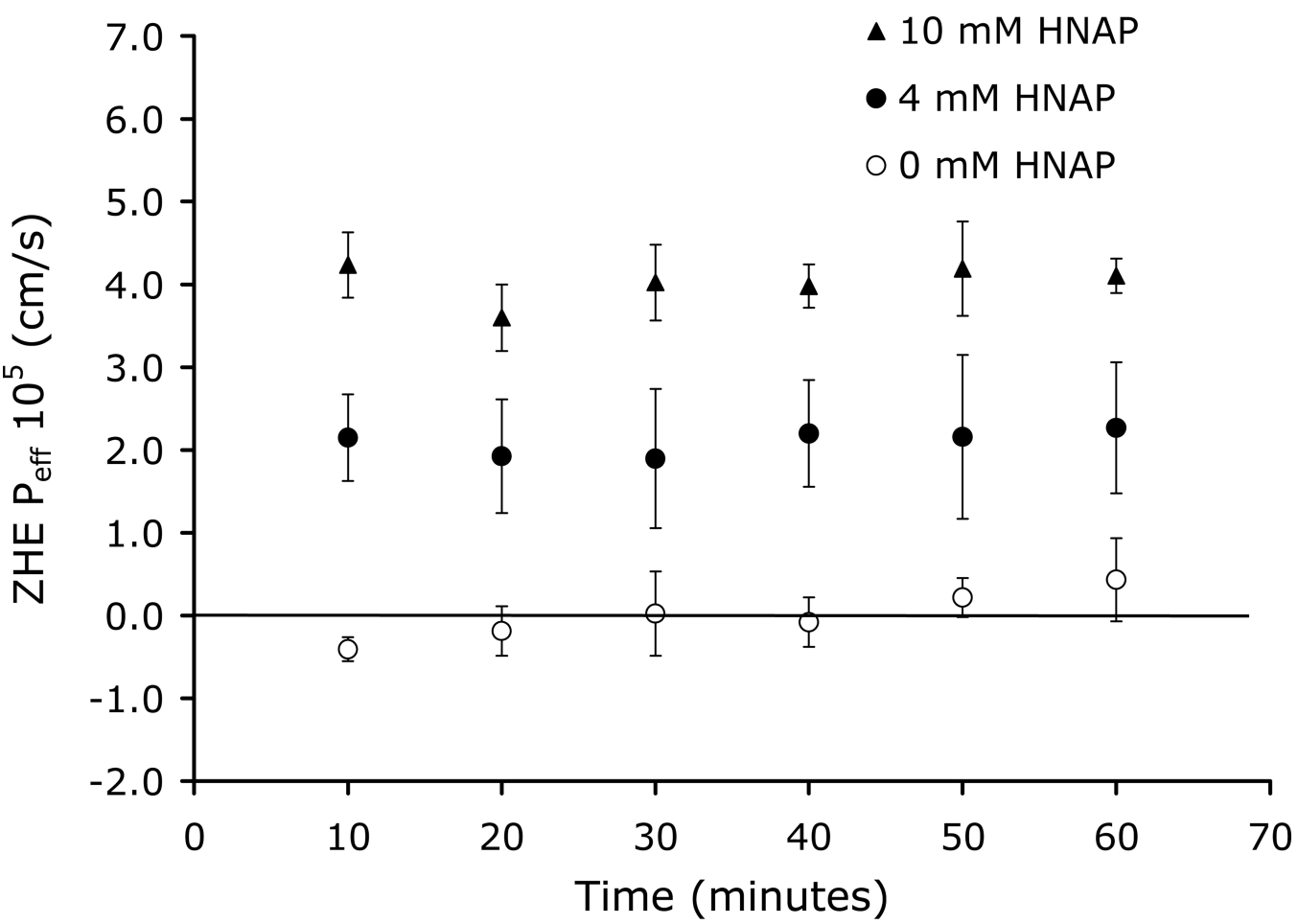

Figure 7.
ZHE P_{eff} versus time in rat jejunal perfusion assay at 0, 4, and 10 mM HNAP concentrations

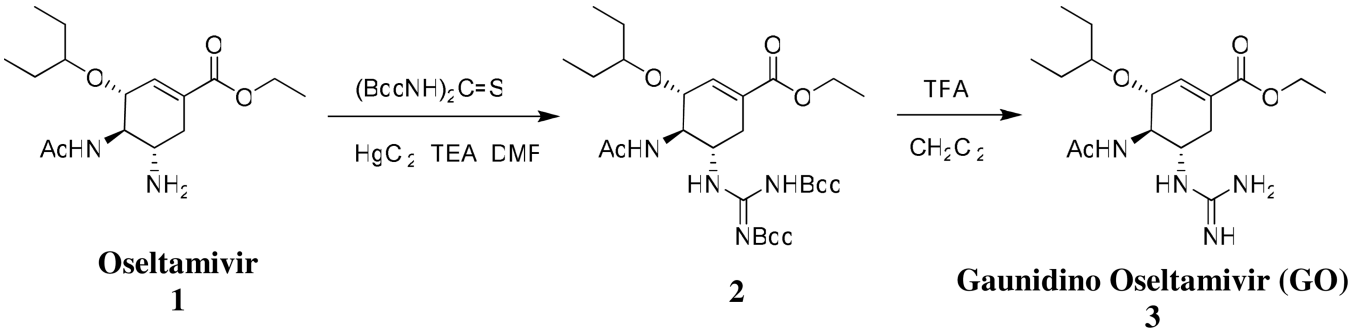

Oseltamivir
1

2

Gaunidino Oseltamivir (GO)
3

Scheme 1.
Chemical Synthesis of Guanidino Oseltamivir

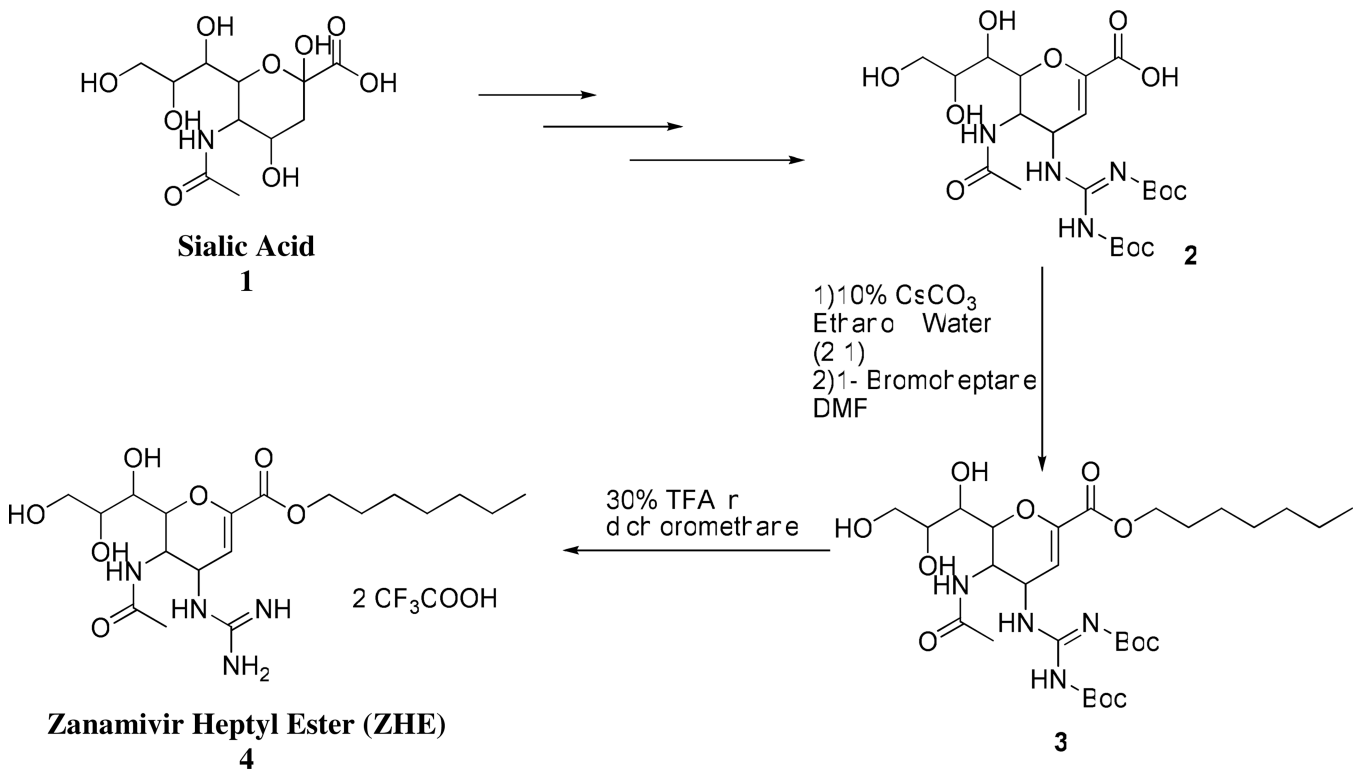

Scheme 2.

Table 1

pK_a, cLogP, and Log D of ZHE, GO, and HNAP

Compound	pK_a	cLog P[a]	Log D (pH 6.5)
Guanidino Oseltamivir (GO)	12.80[a]	0.83	−1.17[a]
Zanamivir HeptylEster (ZHE)	11.26[a]	0.69	−1.31[a]
1-Hydroxy-2-Naphthoic acid (HNAP)	2.70[b]	3.29	0.25[c]

[a]Calculated values using Advanced Chemistry Development (ACD/Labs) Software V8.14.

[b]From reference[29]

[c]From reference[13]

Table 2

Summary of K_{11aq}, K_{11oct}, and Log P_{AB} values determined from octanol-buffer (pH 6.5) partitioning studies and calculated values of percent ion-pair in aqueous solution (%$[AB]_{aq}$) at 1 mM and 10 mM counterion concentration

Ion-pair	K_{11aq} (M^{-1})	K_{11oct} (M^{-1})	Log P_{AB}	%$[AB]_{aq}$ 1 mM	%$[AB]_{aq}$ 10 mM
GO-HNAP	2.91	2.2E+05	4.50	0.3%	2.8%
ZHE-HNAP	388	4.8E+04	1.89	28.0%	79.5%

Table 3

Comparison of K_{11aq}, Log P_{AB}, and rat jejunal P_{eff} (0 mM and 10–12 mM HNAP) for ZHE-HNAP and GO-HNAP ion-pairs

Ion-pair	K_{11aq} (M^{-1})	Log P_{AB}	P_{eff} (10^5 cm/s)		
			0 mM HNAP	6 mM HNAP	10–12 mM HNAP
GO-HNAP	2.91	4.50	−0.2 ± 0.2	ND	−0.2 ± 0.2
ZHE-HNAP	388	1.89	0.0 ± 0.4	2.1 ± 0.7	4.0 ± 0.4